

# Identification of a Dynamical Model of the Latching Mechanism of an Aircraft Hatch Door using the Numerical Algorithms for Subspace State-Space System Identification

Carmine Maria Pappalardo, Antonio Lettieri, Domenico Guida

**Abstract**—In this paper, the main objective is to underline the possibility of identifying simplified mechanical models of complex mechanical systems through the numerical techniques of applied system identification to develop control actions. For this purpose, the system identification theory and, in particular, the Numerical Algorithms for Subspace State-Space System Identification, shortened in N4SID, are employed in this work considering a mathematical model as the test rig instead of using a real system and the data gathered from real sensors. In particular, the mechanical model of the latch system of the ATR 42/72 cargo door is the case study considered in this investigation to integrate the CAD (Computer-Aided Design) model and the dynamical simulations carried out within the MBD (Multi-Body Dynamics) virtual environments. Thus, the software SOLIDWORKS is used for the CAD interface, whereas, at the same time, the software SIMSCAPE is chosen to carry out the numerical simulations of the corresponding multibody model, and the system identification process is performed employing the N4SID suite implemented in MATLAB. When compared with the original nonlinear multibody model, the numerical results found from the dynamical simulations generated in SIMSCAPE, starting from the model developed in SOLIDWORKS, are used to identify a simpler linear dynamical model of the latch system of the hatch door, which could be effectively used in subsequent developments to analyze further the real prototype and for the design of effective control strategies.

**Index Terms**—Computer-Aided Design (CAD), Multi-Body Dynamics (MBD), Integration of Computer-Aided Design and Analysis (I-CAD-A), Numerical Algorithms for Subspace State-Space System Identification (N4SID), Hatch door, Latch system.

## I. INTRODUCTION

This paper deals with developing and identifying a dynamical model of the latching system of an aircraft hatch door through the use of the Numerical Algorithms for Subspace State-Space System Identification (N4SID) combined with the use of an MBD (Multi-Body Dynamics) model developed from a CAD (Computer-Aided Design) drawing. This introduction section poses the problem of interest in this investigation and provides some fundamental background

Manuscript received December 8, 2020; revised February 6, 2021.

Carmine M. Pappalardo is an Assistant Professor at the Department of Industrial Engineering, University of Salerno, Via Giovanni Paolo II, 132, 84084 Fisciano, Salerno, Italy (corresponding author, email: cpappalardo@unisa.it).

Antonio Lettieri is a Researcher at the Spin-Off MEID4 s.r.l., Via Giovanni Paolo II, 132, 84084 Fisciano, Salerno, Italy (email: a.lettieri20@gmail.com).

Domenico Guida is a Full Professor at the Department of Industrial Engineering, University of Salerno, Via Giovanni Paolo II, 132, 84084 Fisciano, Salerno, Italy (email: guida@unisa.it).

material for clarifying the approach adopted throughout this work. A short literature review is also reported in this section to emphasize the importance of the Integration of Computer-Aided Design and Analysis (I-CAD-A) and the potential of applied system identification in engineering applications in general. Finally, the scope and the contributions of the paper are highlighted herein, and the organization of the entire manuscript is explained.

### A. Background Information and Formulation of the Problem of Interest for this Investigation

To properly simulate the dynamic behavior of a general mechanical system, the mechanism under investigation can be modeled with diverse degrees of complexity, and the use of the multibody technique is well suited to describe a wide range of articulated mechanical systems [1], [2]. The system model should be detailed enough to fully describe its dynamics and its peculiar aspects, but, in the meanwhile, an excessive complexity will result in an undesired delay in the duration of the numerical analysis without adding useful information. In this scenario, identifying a simple model of a complex mechanism is of paramount interest to obtain useful tools that can be used for parametric analysis, predictive goals, and control strategies [3]–[6].

The system identification theory and the numerical procedures of applied system identification represent powerful instruments to obtain an input-output black-box model of the desired system, starting from the time evolution of appropriately selected inputs and outputs gathered from sensors during experimental tests on the real system [7], [8]. On the other hand, when designing a new part or when the real systems are not available to be tested, or there is no possibility of running the necessary experiments [9], [10], a virtual prototyping campaign could be carried out [11], [12]. Starting from the CAD model, the integration between the CAD software used to develop the three-dimensional model of the system of interest, and the multibody software needed to analyze it dynamically, become necessary to obtain a virtual prototype suited for the numerical analysis [13], [14]. In this respect, several aspects must be considered, such as the compatibility of the two software and the necessity to use a model that has been properly modified to consider only the bodies necessary to describe the dynamics of the mechanism. Thus, this paper is collocated in this research framework and is devoted to identifying a dynamical model of the latching system of an aircraft hatch door using the numerical algorithms of subspace state-space system identification.

### *B. Literature Review on the Virtual Prototyping and the Integration of Computer-Aided Design and Analysis*

In this subsection, the integration between computer-aided design and computer-aided analysis will be faced and explored to understand its importance. The role of computer design and simulation in modern engineering is fundamental for increasing the quality of the final products and reducing their cost. The process starts from the design phase and then moves to analyze the dynamic and/or static behavior of the mechanical system under investigation [15], [16]. The integration between the different phases of the computer-aided process is not a trivial issue since the design environment and the analysis environment are based on different hypotheses and must be addressed carefully [17]–[19]. Several approaches can be used to solve the integration of computer-aided design and analysis apart from manually modifying the CAD model, which can be relatively easy. Still, this process is also strongly influenced by the engineering experience. However, various techniques for autonomous or partially automated reduction are available in the literature. In [20], Daberkow and Kreuzer described an object-oriented modeling approach to integrate the CAD and the multibody simulations starting from a previous work of Otter et al. [21]. In [22], Thakur et al. presented a list of techniques suitable for physics-based numerical simulations since, for different problems, diverse approaches should be followed. In [23], Shabana proposed a new computer-aided methodology based on the integration of the computer-aided phases of design and analysis regarding the field of multibody vehicle dynamics. Shi et al. developed a continuum-based liquid sloshing approach to consider the effect of interaction between the geometry of the tank and the liquid on the general vehicle dynamics [24]. In [25], Khan and Rezwana suggested an approach based on Hierarchical Data Format, used as a link between the DAE (Differential-Algebraic Equations) and the CAE (Computer-Aided Engineering) systems, while Hamri et al. in [26] proposed a method based on a different shape representation called mixed shape representation to reduce the gaps between the CAD and CAE programs. Another option is to link CAD software like SOLIDWORKS and the multipurpose programming environment MATLAB, which allows importing a CAD model in the simulation environment called SIMSCAPE [27]–[29] and to develop also multi-domain models [30].

Today, the importance of computer-aided engineering along the productive process is essential and cannot be neglected if optimal results are required. Despite its central role, the integration between the designing and simulation phases is not as easy and optimized as possible. The strategy of integration can be very different, for example, the use of a Common Data Model (CDM), where all the information for both design and analysis are store as proposed in [31] by Gujarathi and Ma, a completely different formulation of the geometric features as proposed by Mikkola et al. in [32]. The two phases have different aims, and so they are based on diverse principles, namely the NURBS (Non-Uniform Rational Basis-Spline) for the CAD software and the multibody approach MBD (Multi-Body Dynamics) [33], [34]. The difference between the two kinds of representations is the accuracy with which the surfaces of the model are

described. The model developed during the designing phase needs great accuracy and an appropriate appearance to effectively present the product effectively. On the other hand, the necessities of an analyst are different, and, in particular, the focus is on the parts of the system that play an active role in kinematic and dynamic studies. Moreover, a model composed of an elevate number of bodies would result in requiring a long simulation time and does not necessarily result in a better quality of the outcomes of the simulations. These are the main reasons because of the need for a preliminary phase in which the CAD model will be modified and simplified to get a model suitable for the analysis [35]. In general, as briefly discussed in this paper, the approach based on the integration of computer-aided design and analysis can be effectively employed for developing new continuum-based finite element models for addressing the small and large deformation problems of flexible multibody mechanical systems, as well as for performing a system identification process that leads to the construction of a simplified state-space dynamical model of the mechanical system of interest.

The large diffusion of computers and the development of technology in engineering fields rapidly and actually changed the designing process of a wide variety of items [36]–[38]. The integration of the CAD-CAE environment and the methodology highly driven by computer-aided strategies can be seen in various engineering fields. Approaches based on 3D printing and virtual reality are growing in the domain of civil engineering, and building industry [39], [40], modeling and simulations techniques based on computer-aided approach are applied in vehicle engineering prototyping and design of tires [41], of car components [42], and bicycle frames [43], [44]. The availability of a virtual model of a system will improve the quality of the final result and reduce the necessity to realize several physical prototypes to be tested to validate the project. A large number of virtual tests and numerical simulations can replace physical experiments reducing costs and leading to a more systematic approach to the design and prototyping process itself [45]. The required level of details for the CAD models and the CAE models is clearly different, and the initial concept of a generic system will probably change as the results of simulations and analyses [46]. To avoid a large number of physical prototypes, virtual prototyping can help cut off the duration and cost of the all productive process [47], as discussed in this paper.

### *C. Literature Review on System Identification and Nonlinear Control of Mechanical Systems*

A generic system analysis requires simplifications and diverse hypotheses to explore its characteristics, and different approaches can be followed to address this issue. For analysis purposes, the multibody modeling is well suited to investigate the kinematics and dynamics of a system, but this generally results in complex and nonlinear formulations [48], [49]. Thus, in certain areas where a fast solution is needed as the field of control or hardware-in-the-loop simulations, an alternative formulation is needed [50], [51]. For the possibility to describe a system using a simple input-output numerical formulation, the system identification is a widely used technique in the field of controls, starting from data gathered

from sensors during real experiments or from the results of a numerical simulation [52]. Some diverse techniques and approaches can vary from the specific area of interest or system to analyze, leading to a mathematical formulation suitable for control and parameter identification purposes [53]–[55]. The multibody methodology, on the other hand, is an efficient method which can be applied with confidence to a large variety of mechanical systems, well suited for numerical computer-assisted formulation and to analyze the behavior of the systems under investigation [56]–[58]. In other cases, when the real mechanism is already available, and an experimental campaign can be carried out, it is possible to apply the system identification theory. The works of Ljung [59] and of Juang and Phan [60] give a complete overview of the argument. Using the data collected from experimental tests, it is possible to identify a mathematical model of the system and diverse identification algorithms are available. In particular, in this paper, the focus is on the subspace state-space system identification approach [61]. Application of the system identification are widespread in the field of structural engineering, to perform modal analysis of the system as in [62], where the authors analyze a frame structure and propose a numerical procedure founded on combining the Observer/Kalman Filter Identification Method (OKID) with the Eigensystem Realization Algorithm (ERA) to determine the sequence of the Markov parameters of the system. In [63], Nord et al. used a combination of collected and simulated data to identify the modal parameters and studied the behavior of a lighthouse placed in ice-infested waters. Other examples of the system identification applicability can be found in [64], where the data collected from a real car used as a test rig are used to identify an input-output model of the system. In [65], Zhiyu et al. identified a state-space model of a flexible space manipulator. In the work of Navik et al. [66], an application of the identification procedure can be found applied to railway systems regarding the damping properties of the catenary system. In [67], Yu et al. proposed an optimized neural network for the parameter identification of the proton exchange membrane of fuel cells. In [68], Chen et al. investigated the pulsed eddy current data analysis for the structural health monitoring using linear time-domain models and frequency-domain feature extractions. In [69], Gray et al. solved the nonlinear system identification problem for a multivariable nonlinear input-output system represented in terms of a Chen-Fliess functional expansion. In [70], Wu and Jahanshahi proposed a comprehensive review of the recent issues concerning the data fusion applications in structural health monitoring. In [71], Klus et al. derived a data-driven method for the approximation of the Koopman generator regarded as a straightforward extension of an extended dynamic mode decomposition. In [72], Ljung et al. provided a new summary of the main ideas and results of kernel-based regularization methods for applied system identification. In [73], Bai et al. proposed two recent innovations that extend dynamic mode decomposition to systems with actuation and systems with heavily subsampled measurements. In [74], Zhang et al. developed a two-stage Bayesian formulation for structural system identification taking into account modeling errors of natural mode shapes and frequencies. In [75], Ribeiro et al. focused on the smoothness of optimization problems arising

in the prediction and estimation of error parameters of linear and nonlinear systems. Several works found in the literature on these arguments highlight the interest and the complexity of the problem considered in this investigation.

#### *D. Scope and Contributions of this Study*

In this work, starting from its detailed CAD model and using the system identification theory, the authors defined a simplified model of the latch system of the cargo door of the ATR 42/72. The aim is to show the possibility to use a virtual model instead of the physical one to simulate different cases, gather the outputs of the system in response to user-defined inputs, and finally use them to identify an input-output numerical model of the door using the Numerical Algorithms for Subspace State-Space System Identification (N4SID). To achieve these goals, the complete CAD model of the hatch door is appropriately simplified, particularly focusing on the latch system of the door to use it for the necessary numerical simulations. Thus, the two computer programs, respectively called SOLIDWORKS and MATLAB/SIMSCAPE, are used for CAD modeling and MBD numerical simulations, while a general-purpose MATLAB code developed by the authors by using the N4SID method is employed for identifying a first-order state-space dynamical model of the latch system of interest in the ATR 42/72 cargo door.

In this investigation, the objective is to obtain a simplified dynamical model of the latch system of the ATR 42/72 cargo door using the application of the system identification theory. To this end, a CAD-MBD synergistic interaction results necessary to obtain a detailed model to describe the behavior of the mechanical system under investigation properly. The procedure devised in this work is general and can be easily applied to a wide range of mechanical systems of practical interest. This paper also aims to show how a detailed CAD model can be easily imported in a multibody environment. The MATLAB program called SIMSCAPE, in the present case, analyzes the dynamic behavior of complex mechanisms such as the case study of this work. Furthermore, the multibody model can be used as a substitute for the real mechanism, and several tests can be run faster and more easily compared to a real experimental campaign. The model can also be used for multiple purposes as, for example, defining control strategies for the real system. In this respect, the multibody model cannot be used as it is. Still, a simpler model is required, and the system identification can be a reasonable choice to obtain a simple and efficient mathematical description of the problem. A relatively simple input-output model can be defined and then used to develop real-time controllers. The approach used in this work can be applied to a generic mechanical system for which a CAD model can be created as the starting point of the overall numerical procedure. Finally, to demonstrate the practical use of the identified state-space models of the aircraft subsystem considered in the paper, optimal feedback controllers were designed using the identified model and solving the discrete-time infinite-horizon Riccati algebraic equation. This allowed for performing numerical experiments of the closed-loop dynamics of the state-space systems identified for the latching mechanism in response to an arbitrary excitation, as shown in detail and discussed in the numerical results section of the manuscript.

### E. Organization of the Manuscript

This manuscript is organized considering the following structure. Section II provides the methodology employed in this paper to develop the numerical analysis based on the tools of applied system identification. In Section III, the case study considered in this investigation is described, whereas the numerical results found are reported and discussed thoroughly. Section IV is a conclusive section that contains a summary of the work done in the paper, some conclusions reached in the present analysis, and possible interesting directions for addressing future works.

## II. APPLIED SYSTEM IDENTIFICATION

In this section, the mathematical background and the computational methodology utilized to develop the present research work and analyze the case study considered in this investigation are reported. For this purpose, the fundamental aspects of applied system identification are recalled, paying particular attention to the state-space dynamical models used for describing linear mechanical systems, as well as to the key features of the numerical algorithms employed for performing the subspace state-space system identification.

### A. Linear Dynamical Models of Mechanical Systems

This subsection provides the core equations that mathematically describe linear dynamical systems typically found in mechanical and control engineering applications. A generic linear dynamical model of a mechanical system can be written in the following matrix form:

$$\mathbf{M}\ddot{\mathbf{x}}(t) + \mathbf{R}\dot{\mathbf{x}}(t) + \mathbf{K}\mathbf{x}(t) = \mathbf{F}(t) \quad (1)$$

where the constant matrices  $\mathbf{M}$ ,  $\mathbf{R}$ , and  $\mathbf{K}$  are, respectively, the mass matrix, the damping matrix, and the stiffness matrix of the mechanical system having dimensions  $n_2 \times n_2$ , while the vectors  $\ddot{\mathbf{x}}(t)$ ,  $\dot{\mathbf{x}}(t)$ , and  $\mathbf{x}(t)$  are, respectively, the generalized accelerations, the generalized velocities, and the generalized displacements of the dynamical system having dimension  $n_2$ , being  $n_2$  the degrees of freedom of the system. The vector  $\mathbf{F}(t)$  of dimension  $n_2$  is the generalized vector of the external forces acting on the system. Furthermore, the output vector of the considered mechanical system, identified as  $\mathbf{y}(t)$  with dimension  $m$ , obeys the following mathematical formulation:

$$\mathbf{y}(t) = \mathbf{C}_a\ddot{\mathbf{x}}(t) + \mathbf{C}_v\dot{\mathbf{x}}(t) + \mathbf{C}_d\mathbf{x}(t) \quad (2)$$

where the constant matrices  $\mathbf{C}_a$ ,  $\mathbf{C}_v$ , and  $\mathbf{C}_d$  having dimensions  $m \times n_2$  are the output influence matrices related to the generalized accelerations, velocities, and displacements, respectively.

From the linear matrix form of the system model, a state-space formulation can be easily obtained. To achieve this objective, the first step is the construction of the state vector of the mechanical system denoted with  $\mathbf{z}(t)$  with dimension  $n = 2n_2$ , which is defined as follows:

$$\mathbf{z}(t) = \begin{bmatrix} \mathbf{x}(t) \\ \dot{\mathbf{x}}(t) \end{bmatrix} \quad (3)$$

Then, defining as  $\mathbf{u}(t)$  the input vector of the dynamical system having dimension  $r$ , the state-space model in the

continuous-time domain can be written as follows:

$$\begin{cases} \dot{\mathbf{z}}(t) = \mathbf{A}_c\mathbf{z}(t) + \mathbf{B}_c\mathbf{u}(t) \\ \mathbf{y}(t) = \mathbf{C}\mathbf{z}(t) + \mathbf{D}\mathbf{u}(t) \end{cases} \quad (4)$$

where  $\mathbf{A}_c$  and  $\mathbf{B}_c$  are, respectively, the continuous-time state matrix of dimensions  $n \times n$  and the continuous-time input influence matrix of dimensions  $n \times r$ , whereas  $\mathbf{C}$  and  $\mathbf{D}$  are, respectively, the output influence matrix of dimensions  $m \times n$  and the direct transmission matrix of dimensions  $m \times r$ . These matrices have the following structure:

$$\mathbf{A}_c = \begin{bmatrix} \mathbf{O} & \mathbf{I} \\ -\mathbf{M}^{-1}\mathbf{K} & -\mathbf{M}^{-1}\mathbf{R} \end{bmatrix}, \quad \mathbf{B}_c = \begin{bmatrix} \mathbf{O} \\ \mathbf{M}^{-1}\mathbf{B}_f \end{bmatrix} \quad (5)$$

$$\mathbf{C} = \begin{bmatrix} \mathbf{C}_d - \mathbf{C}_a\mathbf{M}^{-1}\mathbf{K} & \mathbf{C}_v - \mathbf{C}_a\mathbf{M}^{-1}\mathbf{R} \end{bmatrix} \quad (6)$$

$$\mathbf{D} = \mathbf{C}_a\mathbf{M}^{-1}\mathbf{B}_f \quad (7)$$

where  $\mathbf{O}$  is the null matrix,  $\mathbf{I}$  is the identity matrix, and  $\mathbf{B}_f$  is the influence matrix having dimensions  $n_2 \times r$  that defines the location and the type of the inputs as stated by the following equation:

$$\mathbf{F}(t) = \mathbf{B}_f\mathbf{u}(t) \quad (8)$$

As mentioned before, the state-space model described above is valid in the continuous-time domain. However, the related discrete-time model is obtained in general from the use of subspace state-space system identification procedures. Identifying the continuous-time model can be easily obtained as the result of a transformation of the identified discrete-time dynamical model. Thus, the discrete-time state-space model of a generic mechanical system can be written as follows:

$$\begin{cases} \mathbf{z}(k+1) = \mathbf{A}_d\mathbf{z}(k) + \mathbf{B}_d\mathbf{u}(k) \\ \mathbf{y}(k) = \mathbf{C}\mathbf{z}(k) + \mathbf{D}\mathbf{u}(k) \end{cases} \quad (9)$$

where  $k$  is the discrete time,  $\mathbf{z}(k)$  denotes the discrete-time state vector of dimension  $n$ ,  $\mathbf{u}(k)$  identifies the discrete-time input vector of dimension  $r$ ,  $\mathbf{y}(k)$  indicates the discrete-time output vector of dimension  $m$ ,  $\mathbf{A}_d$  is the state matrix of the discrete-time system of dimensions  $n \times n$ ,  $\mathbf{B}_d$  indicates the input influence matrix of the discrete-time system of dimensions  $n \times r$ ,  $\mathbf{C}$  identifies the output influence matrix of the dynamical system of dimensions  $m \times n$ , and  $\mathbf{D}$  indicates the direct transmission matrix of the dynamical system of dimensions  $m \times r$ . Note that, because of the manner they are defined, the matrices  $\mathbf{C}$  and  $\mathbf{D}$  are identical in both the continuous-time and discrete-time domains. Therefore, no transformation is needed, in this case, since the measurement equations form a set of algebraic equations.

### B. Numerical Algorithms for Subspace State-Space System Identification

This subsection describes the main calculation phases of the numerical algorithms for subspace state-space system identification, shortened with the acronym N4SID. For this purpose, consider the representation of the discrete-time space-state model of a general linear mechanical system defined using the dynamic and measurement equations given by Equation (9). In these equations, as mentioned before,  $k$  stands for the discrete-time variable, while the matrices  $\mathbf{A}_d$  and  $\mathbf{B}_d$  are, respectively, the discrete-time state matrix

and the discrete-time input influence matrix. The first-order dynamic equations and the measurement equations forming the discrete-time state-space model given by Equation (9) can be formulated in a different matrix form as follows:

$$\begin{cases} \mathbf{Y}_p = \mathbf{\Gamma}_i \mathbf{Z}_p + \mathbf{H}_i \mathbf{U}_p \\ \mathbf{Y}_f = \mathbf{\Gamma}_i \mathbf{Z}_f + \mathbf{H}_i \mathbf{U}_f \\ \mathbf{Z}_f = \mathbf{A}_d^i \mathbf{Z}_p + \mathbf{\Delta}_i \mathbf{U}_p \end{cases} \quad (10)$$

where  $i$  and  $j$  are appropriate integer numbers,  $l$  represents the length of the data record sampled in the discrete-time domain,  $\mathbf{\Gamma}_i$  (size  $mi \times n$ ) is the system observability matrix,  $\mathbf{\Delta}_i$  (size  $n \times ri$ ) is the system controllability matrix,  $\mathbf{H}_i$  (size  $mi \times ri$ ) represents the triangular Toeplitz matrix associated with the discrete-time state-space model, while the matrices  $\mathbf{U}_p$  (size  $i \times jr$ ),  $\mathbf{U}_f$  (size  $i \times jr$ ),  $\mathbf{Y}_p$  (size  $i \times jl$ ), and  $\mathbf{Y}_f$  (size  $i \times jl$ ) are, respectively, the Hankel matrix of the past and future inputs, as well as the Hankel matrix of the past and future outputs. These discrete-time matrices can be easily constructed from the input and output data, respectively recorded in the vectors  $\mathbf{u}(k)$  and  $\mathbf{y}(k)$ , as follows:

$$\mathbf{U}_p = \begin{bmatrix} \mathbf{u}(0) & \mathbf{u}(1) & \dots & \mathbf{u}(j-1) \\ \mathbf{u}(1) & \mathbf{u}(2) & \dots & \mathbf{u}(j) \\ \vdots & \vdots & \ddots & \vdots \\ \mathbf{u}(i-1) & \mathbf{u}(i) & \dots & \mathbf{u}(i+j-2) \end{bmatrix} \quad (11)$$

$$\mathbf{U}_f = \begin{bmatrix} \mathbf{u}(i) & \mathbf{u}(i+1) & \dots & \mathbf{u}(i+j-1) \\ \mathbf{u}(i+1) & \mathbf{u}(i+2) & \dots & \mathbf{u}(i+j) \\ \vdots & \vdots & \ddots & \vdots \\ \mathbf{u}(2i-1) & \mathbf{u}(2i) & \dots & \mathbf{u}(2i+j-2) \end{bmatrix} \quad (12)$$

$$\mathbf{Y}_p = \begin{bmatrix} \mathbf{y}(0) & \mathbf{y}(1) & \dots & \mathbf{y}(j-1) \\ \mathbf{y}(1) & \mathbf{y}(2) & \dots & \mathbf{y}(j) \\ \vdots & \vdots & \ddots & \vdots \\ \mathbf{y}(i-1) & \mathbf{y}(i) & \dots & \mathbf{y}(i+j-2) \end{bmatrix} \quad (13)$$

$$\mathbf{Y}_f = \begin{bmatrix} \mathbf{y}(i) & \mathbf{y}(i+1) & \dots & \mathbf{y}(i+j-1) \\ \mathbf{y}(i+1) & \mathbf{y}(i+2) & \dots & \mathbf{y}(i+j) \\ \vdots & \vdots & \ddots & \vdots \\ \mathbf{y}(2i-1) & \mathbf{y}(2i) & \dots & \mathbf{y}(2i+j-2) \end{bmatrix} \quad (14)$$

The parameters  $i$  and  $j$  have been chosen arbitrarily, bearing in mind that the higher they are, the more accurate the identification will be having more data available. The terms  $\mathbf{Z}_p$  (size  $n \times j$ ) and  $\mathbf{Z}_f$  (size  $n \times j$ ) respectively represent the sequences of past and future states, and are defined as follows:

$$\mathbf{Z}_p = [ \mathbf{z}(0) \quad \mathbf{z}(1) \quad \dots \quad \mathbf{z}(j-1) ] \quad (15)$$

$$\mathbf{Z}_f = [ \mathbf{z}(i) \quad \mathbf{z}(i+1) \quad \dots \quad \mathbf{z}(i+j-1) ] \quad (16)$$

As already mentioned above, the matrix denoted with  $\mathbf{\Gamma}_i$  represents the observability matrix and is defined as:

$$\mathbf{\Gamma}_i = \begin{bmatrix} \mathbf{C} \\ \mathbf{CA}_d \\ \mathbf{CA}_d^2 \\ \vdots \\ \mathbf{CA}_d^{i-1} \end{bmatrix} \quad (17)$$

The matrix denoted with  $\mathbf{\Delta}_i$  represents the controllability matrix and is defined as:

$$\mathbf{\Delta}_i = [ \mathbf{A}_d^{i-1} \mathbf{B}_d \quad \mathbf{A}_d^{i-2} \mathbf{B}_d \quad \dots \quad \mathbf{A}_d \mathbf{B}_d \quad \mathbf{B}_d ] \quad (18)$$

The matrix  $\mathbf{H}_i$  represents the triangular Toeplitz matrix and is defined as follows:

$$\mathbf{H}_i = \begin{bmatrix} \mathbf{D} & \mathbf{O} & \mathbf{O} & \dots & \mathbf{O} \\ \mathbf{CB}_d & \mathbf{D} & \mathbf{O} & \dots & \mathbf{O} \\ \mathbf{CA}_d \mathbf{B}_d & \mathbf{CB}_d & \mathbf{D} & \dots & \mathbf{O} \\ \vdots & \vdots & \vdots & \ddots & \vdots \\ \mathbf{CA}_d^{i-2} \mathbf{B}_d & \mathbf{CA}_d^{i-3} \mathbf{B}_d & \mathbf{CA}_d^{i-4} \mathbf{B}_d & \dots & \mathbf{D} \end{bmatrix} \quad (19)$$

By properly manipulating Equation (10), one can find that matrix  $\mathbf{Z}_f$  can be written as a linear combination of the matrices  $\mathbf{U}_p$  and  $\mathbf{Y}_p$  as follows:

$$\begin{aligned} \mathbf{Z}_f &= \mathbf{A}_d^i \mathbf{Z}_p + \mathbf{\Delta}_i \mathbf{U}_p \\ &= \mathbf{A}_d^i (\mathbf{\Gamma}_i^+ \mathbf{Y}_p - \mathbf{\Gamma}_i^+ \mathbf{H}_i \mathbf{U}_p) + \mathbf{\Delta}_i \mathbf{U}_p \\ &= (\mathbf{\Delta}_i - \mathbf{A}_d^i \mathbf{\Gamma}_i^+ \mathbf{H}_i) \mathbf{U}_p + \mathbf{A}_d^i \mathbf{\Gamma}_i^+ \mathbf{Y}_p \\ &= \mathbf{L}_p \mathbf{W}_p \end{aligned} \quad (20)$$

where the plus superscript indicates the Moore-Penrose pseudo-inverse matrix, while the matrices  $\mathbf{L}_p$  and  $\mathbf{W}_p$  can be written as follows:

$$\mathbf{L}_p = [ \mathbf{\Delta}_i - \mathbf{A}_d^i \mathbf{\Gamma}_i^+ \mathbf{H}_i \quad \mathbf{A}_d^i \mathbf{\Gamma}_i^+ ], \quad \mathbf{W}_p = \begin{bmatrix} \mathbf{U}_p \\ \mathbf{Y}_p \end{bmatrix} \quad (21)$$

By combining Equation (20) with Equation (10), one can write the future output vector as:

$$\mathbf{Y}_f = \mathbf{\Gamma}_i \mathbf{Z}_f + \mathbf{H}_i \mathbf{U}_f = \mathbf{\Gamma}_i \mathbf{L}_p \mathbf{W}_p + \mathbf{H}_i \mathbf{U}_f \quad (22)$$

At this stage, define  $\mathbf{\Pi}_{\mathbf{U}_f^\perp}$  as the projection matrix onto the set of future inputs as:

$$\mathbf{\Pi}_{\mathbf{U}_f^\perp} = \mathbf{I} - \mathbf{U}_f^T (\mathbf{U}_f \mathbf{U}_f^T)^+ \mathbf{U}_f \quad (23)$$

By post-multiplying Equation (22) with the projection matrix onto the set of future inputs  $\mathbf{\Pi}_{\mathbf{U}_f^\perp}$ , one obtains:

$$\mathbf{Y}_f \mathbf{\Pi}_{\mathbf{U}_f^\perp} = \mathbf{\Gamma}_i \mathbf{L}_p \mathbf{W}_p \mathbf{\Pi}_{\mathbf{U}_f^\perp} + \mathbf{H}_i \mathbf{U}_f \mathbf{\Pi}_{\mathbf{U}_f^\perp} \quad (24)$$

which leads to:

$$\mathbf{Y}_f \mathbf{\Pi}_{\mathbf{U}_f^\perp} = \mathbf{\Gamma}_i \mathbf{L}_p \mathbf{W}_p \mathbf{\Pi}_{\mathbf{U}_f^\perp}, \quad \mathbf{H}_i \mathbf{U}_f \mathbf{\Pi}_{\mathbf{U}_f^\perp} = \mathbf{O} \quad (25)$$

For simplicity, let  $\bar{\mathbf{W}}_p$  be the following matrix:

$$\bar{\mathbf{W}}_p = (\mathbf{W}_p \mathbf{\Pi}_{\mathbf{U}_f^\perp})^+ \mathbf{W}_p \quad (26)$$

Post-multiplying both members of Equation (25) by  $\bar{\mathbf{W}}_p$  yields:

$$\mathbf{Y}_f \mathbf{\Pi}_{\mathbf{U}_f^\perp} \bar{\mathbf{W}}_p = \mathbf{\Gamma}_i \mathbf{L}_p \mathbf{W}_p \mathbf{\Pi}_{\mathbf{U}_f^\perp} \bar{\mathbf{W}}_p \quad (27)$$

where:

$$\begin{aligned} \mathbf{\Gamma}_i \mathbf{L}_p \mathbf{W}_p \mathbf{\Pi}_{\mathbf{U}_f^\perp} \bar{\mathbf{W}}_p &= \mathbf{\Gamma}_i \mathbf{L}_p \mathbf{W}_p \mathbf{\Pi}_{\mathbf{U}_f^\perp} (\mathbf{W}_p \mathbf{\Pi}_{\mathbf{U}_f^\perp})^+ \mathbf{W}_p \\ &= \mathbf{\Gamma}_i \mathbf{L}_p \mathbf{W}_p \mathbf{\Pi}_{\mathbf{U}_f^\perp} \mathbf{\Pi}_{\mathbf{U}_f^\perp}^+ \mathbf{W}_p^+ \mathbf{W}_p \\ &= \mathbf{\Gamma}_i \mathbf{L}_p \mathbf{W}_p = \mathbf{O}_i \end{aligned} \quad (28)$$

It follows that:

$$\mathbf{O}_i = \mathbf{Y}_f \mathbf{\Pi}_{\mathbf{U}_f^+} \bar{\mathbf{W}}_p = \mathbf{Y}_f \mathbf{\Pi}_{\mathbf{U}_f^+} \left( \mathbf{W}_p \mathbf{\Pi}_{\mathbf{U}_f^+} \right)^+ \mathbf{W}_p \quad (29)$$

and

$$\mathbf{O}_i = \mathbf{\Gamma}_i \mathbf{L}_p \mathbf{W}_p = \mathbf{\Gamma}_i \mathbf{Z}_f, \quad \mathbf{Z}_f = \mathbf{L}_p \mathbf{W}_p \quad (30)$$

In short:

$$\mathbf{O}_i = \mathbf{\Gamma}_i \mathbf{Z}_f \quad (31)$$

From the previous algebraic manipulations, it is apparent that one can directly employ the input and output values of the data record for constructing the matrix  $\mathbf{O}_i$  (size  $li \times j$ ). Besides, one can proceed by multiplying the matrix  $\mathbf{O}_i$  by the weighting matrices  $\mathbf{W}_1$  (size  $li \times li$ ) and  $\mathbf{W}_2$  (size  $j \times j$ ), that will be subsequently defined below, and perform a singular value decomposition of the obtained matrix as follows:

$$\bar{\mathbf{O}}_i = \mathbf{W}_1 \mathbf{O}_i \mathbf{W}_2 = \mathbf{U} \mathbf{\Sigma} \mathbf{V}^T \quad (32)$$

where the rectangular matrix  $\mathbf{\Sigma}$  contains the singular values of the resulting weighted matrix  $\bar{\mathbf{O}}_i$  (size  $li \times j$ ), while the columns of the matrices  $\mathbf{U}$  and  $\mathbf{V}$  form orthonormal vectors. Thus, one can partition the weighted matrix  $\bar{\mathbf{O}}_i$  as follows:

$$\bar{\mathbf{O}}_i = \begin{bmatrix} \mathbf{U}_1 & \mathbf{U}_2 \end{bmatrix} \begin{bmatrix} \mathbf{\Sigma}_1 & \mathbf{O} \\ \mathbf{O} & \mathbf{O} \end{bmatrix} \begin{bmatrix} \mathbf{V}_1^T \\ \mathbf{V}_2^T \end{bmatrix} = \mathbf{U}_1 \mathbf{\Sigma}_1 \mathbf{V}_1^T \quad (33)$$

where  $\mathbf{U}_1$ ,  $\mathbf{U}_2$ ,  $\mathbf{V}_1$ , and  $\mathbf{V}_2$  are submatrices of appropriate dimensions which respectively form the matrices  $\mathbf{U}$  and  $\mathbf{V}$  that appear in the singular value decomposition of the matrix  $\bar{\mathbf{O}}_i$ , while the submatrix  $\mathbf{\Sigma}_1$  is a square diagonal matrix defined as:

$$\mathbf{\Sigma}_1 = \text{diag}(\sigma_1, \sigma_2, \dots, \sigma_{\hat{n}}) \quad (34)$$

where  $\hat{n}$  is the number of the nonzero singular values denoted with  $\sigma_s$ ,  $s = 1, 2, \dots, \hat{n}$ . An in-depth analysis of the spectrum of singular values  $\sigma_s$ ,  $s = 1, 2, \dots, \hat{n}$  of the matrix  $\mathbf{\Sigma}_1$  allows for the determination of the order of the identified space-state model, that is also equal to  $\hat{n}$ . On the other hand, the matrix  $\mathbf{O}_i$  can be explicitly written as follows:

$$\mathbf{O}_i = \mathbf{W}_1^{-1} \mathbf{U}_1 \mathbf{\Sigma}_1 \mathbf{V}_1^T \mathbf{W}_2^{-1} \quad (35)$$

As the next step, considering Equation (31) in conjunction with Equation (35) leads to:

$$\mathbf{O}_i = \mathbf{W}_1^{-1} \mathbf{U}_1 \mathbf{\Sigma}_1 \mathbf{V}_1^T \mathbf{W}_2^{-1} = \mathbf{\Gamma}_i \mathbf{Z}_f \quad (36)$$

Introducing an appropriate non-singular square matrix denoted with  $\mathbf{T}$  of dimensions  $\hat{n} \times \hat{n}$ , Equation (36) can be separated into two parts as follows:

$$\begin{cases} \mathbf{\Gamma}_i = \mathbf{W}_1^{-1} \mathbf{U}_1 \mathbf{\Sigma}_1^{1/2} \mathbf{T} \\ \mathbf{Z}_f = \mathbf{T}^{-1} \mathbf{\Sigma}_1^{1/2} \mathbf{V}_1^T \mathbf{W}_2^{-1} \end{cases} \quad (37)$$

Subsequently, for simplicity, one can consider the  $\mathbf{T}$  matrix as an identity matrix through a similarity transformation. For the above, one can, therefore, calculate the matrices  $\mathbf{\Gamma}_i$  and  $\mathbf{Z}_f$  as:

$$\begin{cases} \mathbf{Z}_f = \mathbf{\Sigma}_1^{1/2} \mathbf{V}_1^T \mathbf{W}_2^{-1} \\ \mathbf{\Gamma}_i = \mathbf{W}_1^{-1} \mathbf{U}_1 \mathbf{\Sigma}_1^{1/2} \end{cases} \quad (38)$$

One can now proceed to determine the identified discrete-time space-state matrices  $\mathbf{A}_d$ ,  $\mathbf{B}_d$ ,  $\mathbf{C}$ , and  $\mathbf{D}$ . First, the identified matrix  $\mathbf{C}$  can be determined directly by extracting the first  $m$  rows of the matrix  $\mathbf{\Gamma}_i$  obtained from the previous

algebraic manipulations. Then, the identified discrete-time state matrix  $\mathbf{A}_d$  can be obtained as follows:

$$\mathbf{\Gamma}_i \mathbf{A}_d = \bar{\mathbf{\Gamma}}_i \Rightarrow \mathbf{A}_d = (\mathbf{\Gamma}_i)^+ \bar{\mathbf{\Gamma}}_i \quad (39)$$

where the matrix  $(\mathbf{\Gamma}_i)^+$  represents the Moore-Penrose pseudo-inverse of the matrix  $\mathbf{\Gamma}_i$ ,  $\bar{\mathbf{\Gamma}}_i$  (size  $m(i-1) \times n$ ) is the matrix  $\mathbf{\Gamma}_i$  in which the last matrix block has been removed from, i.e. the last  $m$  lines, while  $\bar{\mathbf{\Gamma}}_i$  (size  $m(i-1) \times n$ ) is the matrix  $\mathbf{\Gamma}_i$  whose first matrix block has been removed, i.e. the first  $m$  lines. These matrices are given by:

$$\mathbf{\Gamma}_i = \begin{bmatrix} \mathbf{C} \\ \mathbf{C} \mathbf{A}_d \\ \mathbf{C} \mathbf{A}_d^2 \\ \vdots \\ \mathbf{C} \mathbf{A}_d^{i-2} \end{bmatrix}, \quad \bar{\mathbf{\Gamma}}_i = \begin{bmatrix} \mathbf{C} \mathbf{A}_d \\ \mathbf{C} \mathbf{A}_d^2 \\ \mathbf{C} \mathbf{A}_d^3 \\ \vdots \\ \mathbf{C} \mathbf{A}_d^{i-1} \end{bmatrix} \quad (40)$$

Now, to determine the identified  $\mathbf{B}_d$  and  $\mathbf{D}$  matrices, one can consider Equation (10) and multiply both the left and right sides respectively by  $\mathbf{U}_f^+$  and  $\mathbf{\Gamma}_i^\perp$  as follows:

$$\mathbf{\Gamma}_i^\perp \mathbf{Y}_f \mathbf{U}_f^+ = \mathbf{\Gamma}_i^\perp \mathbf{\Gamma}_i \mathbf{Z}_f \mathbf{U}_f^+ + \mathbf{\Gamma}_i^\perp \mathbf{H}_i \mathbf{U}_f \mathbf{U}_f^+ \quad (41)$$

where the matrix  $\mathbf{U}_f^+$  is the Moore-Penrose pseudo-inverse of the matrix  $\mathbf{U}_f$ , while the matrix  $\mathbf{\Gamma}_i^\perp$  is a full rank matrix that satisfies the following equation:

$$\mathbf{\Gamma}_i^\perp \mathbf{\Gamma}_i = \mathbf{O} \quad (42)$$

Having said that, one gets:

$$\mathbf{\Gamma}_i^\perp \mathbf{Y}_f \mathbf{U}_f^+ = \mathbf{\Gamma}_i^\perp \mathbf{H}_i \quad (43)$$

For simplicity of notation, denote the matrix resulting at the left-hand side of Equation (43) with  $\mathbf{N}$  (size  $(li-n) \times mi$ ) and denote the matrix  $\mathbf{\Gamma}_i^\perp$  with  $\mathbf{P}$  (size  $(li-n) \times li$ ). That is:

$$\mathbf{N} = \mathbf{\Gamma}_i^\perp \mathbf{Y}_f \mathbf{U}_f^+, \quad \mathbf{P} = \mathbf{\Gamma}_i^\perp \quad (44)$$

Using this simplified notation, Equation (43) can then be rewritten as:

$$\mathbf{N} = \mathbf{P} \mathbf{H}_i \quad (45)$$

This matrix equation can be expanded as follows:

$$\begin{bmatrix} \mathbf{N}_1 & \mathbf{N}_2 & \dots & \mathbf{N}_i \end{bmatrix} = \begin{bmatrix} \mathbf{P}_1 & \mathbf{P}_2 & \dots & \mathbf{P}_i \end{bmatrix} \mathbf{H}_i \quad (46)$$

The previous matrix equation leads to:

$$\begin{bmatrix} \mathbf{N}_1 \\ \mathbf{N}_2 \\ \vdots \\ \mathbf{N}_i \end{bmatrix} = \begin{bmatrix} \mathbf{P}_1 & \mathbf{P}_2 & \dots & \mathbf{P}_i \\ \mathbf{P}_2 & \mathbf{P}_3 & \dots & \mathbf{O} \\ \vdots & \vdots & \ddots & \vdots \\ \mathbf{P}_i & \mathbf{O} & \dots & \mathbf{O} \end{bmatrix} \begin{bmatrix} \mathbf{I} & \mathbf{O} \\ \mathbf{O} & \mathbf{\Gamma}_i \end{bmatrix} \mathbf{\Omega} \quad (47)$$

where:

$$\mathbf{\Omega} = \begin{bmatrix} \mathbf{D} \\ \mathbf{B}_d \end{bmatrix} \quad (48)$$

It follows that:

$$\mathbf{\Omega} = \begin{bmatrix} \mathbf{I} & \mathbf{O} \\ \mathbf{O} & \mathbf{\Gamma}_i \end{bmatrix}^+ \begin{bmatrix} \mathbf{P}_1 & \mathbf{P}_2 & \dots & \mathbf{P}_i \\ \mathbf{P}_2 & \mathbf{P}_3 & \dots & \mathbf{O} \\ \vdots & \vdots & \ddots & \vdots \\ \mathbf{P}_i & \mathbf{O} & \dots & \mathbf{O} \end{bmatrix}^+ \begin{bmatrix} \mathbf{N}_1 \\ \mathbf{N}_2 \\ \vdots \\ \mathbf{N}_i \end{bmatrix} \quad (49)$$

Once the matrix  $\mathbf{\Omega}$  containing both the matrices  $\mathbf{D}$  and  $\mathbf{B}_d$  is identified, the first  $m$  rows of this matrix correspond

to  $\mathbf{D}$  and the last  $n$  rows correspond to  $\mathbf{B}_d$ .

A focal point of the identification process with the N4SID method is the choice of weighting matrices,  $\mathbf{W}_1$  and  $\mathbf{W}_2$ , that act as a data filter. By selecting the data useful for the identification, these matrices play a central role, thereby generating a significant variation of the singular value decomposition. As the weighting matrices vary, the identification outcome can vary significantly. For this purpose, there is no method that is clearly better than the others. Still, depending on the case, the choice of weighting matrices allows for better or worse identification of the consequent numerical results. In general, there are various types of weighting matrices, and two of these are typically implemented in computer programs. These are referred to as the MOESP (Multivariable Output-Error State sPace) method and the CVA (Canonical Variate Analysis) method.

In the case of the MOESP method, the weighting matrices are given by:

$$\text{MOESP} : \begin{cases} \mathbf{W}_1 = \mathbf{I} \\ \mathbf{W}_2 = \mathbf{\Pi}_{\mathbf{U}_f^\perp} \end{cases} \quad (50)$$

As mentioned before, MOESP is the acronym for “Multivariable Output-Error State sPace”, a methodology implemented by Verhaegen with the LQ decomposition method [7]. For the purposes of determining the order of the identified system  $\hat{n}$ , only the projections of the row space of the matrix  $\mathbf{O}_i$  on the orthogonal complement of the row space of the matrix  $\mathbf{U}_f$  are considered.

In the case of the CVA method, the weighting matrices are given by:

$$\text{CVA} : \begin{cases} \mathbf{W}_1 = \left( E \left[ \left( \mathbf{Y}_f \mathbf{\Pi}_{\mathbf{U}_f^\perp} \right) \left( \mathbf{Y}_f \mathbf{\Pi}_{\mathbf{U}_f^\perp} \right)^T \right] \right)^{-1/2} \\ \mathbf{W}_2 = \mathbf{\Pi}_{\mathbf{U}_f^\perp} \end{cases} \quad (51)$$

where  $E[x]$  represents the expected value of the variable  $x$ . The CVA implemented by Larimore [7], an acronym for “Canonical Variate Analysis”, considers the canonical correlations between the matrix of the past  $\mathbf{W}_p$  in relation to the future inputs  $\mathbf{U}_f$ , and the future outputs  $\mathbf{Y}_f$  in relation to future inputs  $\mathbf{U}_f$ .

### III. NUMERICAL RESULTS AND DISCUSSION

In this section, the analyzed system and the numerical results of the dynamical simulations are presented. To this end, first, the description of the case study is provided. Then, the numerical results arising from the dynamical analysis and the state-space model identification are reported. Finally, an overall discussion on the numerical results found is given.

#### A. Case Study Description

The system chosen for carrying out the numerical analysis is the hatch door of an ATR 42/72 cargo shown in Figure 1.

Thus, the hatch door represents the principal mechanical system considered as the case study. Three main subsystems form the hatch door as a whole: the locking system, the latching system, and the lifting system. In particular, this work focuses on the latching mechanism that allows for disengaging the latches to open the door. As specified in

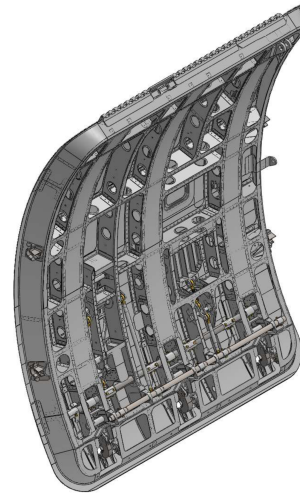


Fig. 1. ATR 42/72 cargo hatch door.

the circular CS25.783 of the Federal Aviation Administration (FAA), the latching mechanism has an important role in assuring a safe closing and opening of the door, thereby preventing unexpected behavior. Therefore, it must be carefully analyzed in the engineering design. A simplified CAD model of the latching mechanism is shown in Figure 2.

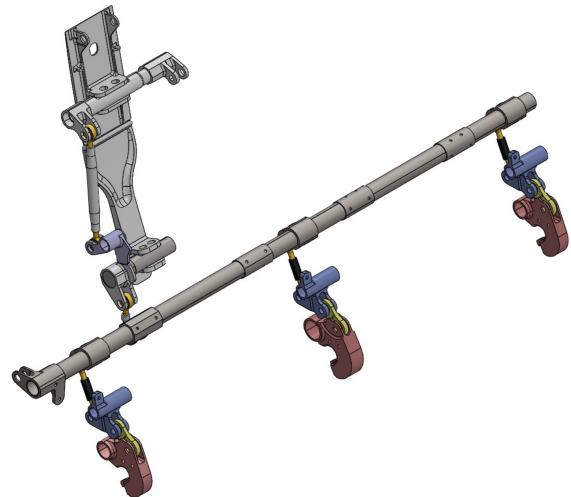


Fig. 2. Latching mechanism CAD model.

The essential elements of the latching mechanism are the three latches, namely three hooks hinged to the lower part of the door. They are connected to a system of rods, cranks, and other mechanical devices, which are controlled through a handle that allows for achieving a synchronized rotation of the different parts. Starting from the complete three-dimensional CAD model of the hatch door, the CAD model of the latching mechanism is simplified and imported in MATLAB, leading to an accurate MBD model that is useful for analyzing its kinematic and dynamical behavior through the use of SIMSCAPE. In particular, in the complete CAD model of the cargo door, all the unnecessary elements for the dynamic analysis of the latching mechanism were removed before the porting from SOLIDWORKS to MATLAB/SIMSCAPE. The resulting MBD model of the latching mechanism is shown in Figure 3.

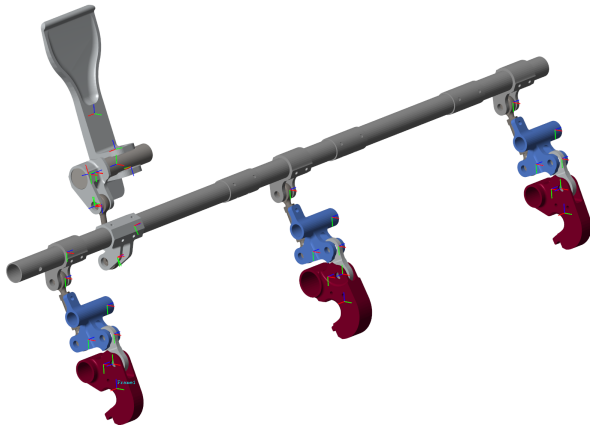


Fig. 3. Latching mechanism MBD model.

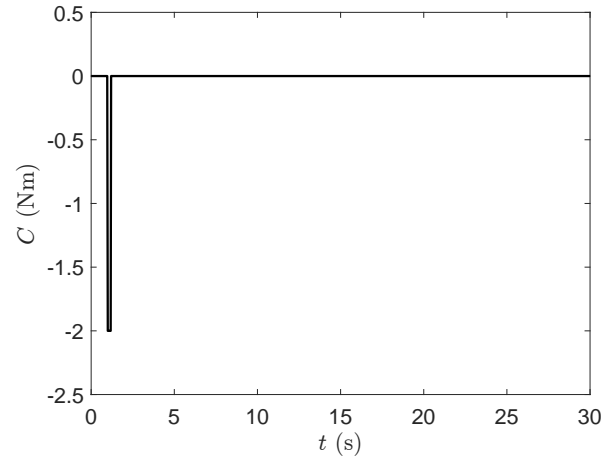
Because of the complexity of the latching mechanism, the block model typical of SIMSCAPE is not reported herein. To properly simulate the dynamical behavior of the latching mechanism, it is necessary to make some hypotheses on the limitations to the motion of the diverse components of the system, particularly regarding the handle and the latches. Besides, the contact or the interference between the mechanical parts of the door is not included in the multibody model studied here since it is not involved in the dynamic analysis. To this end, it is necessary to define a limit range to the rotation of the handle and the latches to reproduce their physical limits. To limit the motion of these components, the function called Limits of the revolute joint available in SIMSCAPE was used. By doing so, a penalty function to impose upper and lower limits on the rotation of the handle of the latches was set. This is necessary to obtain reasonable results from the dynamical simulations and avoid configurations that cannot be reached by the real physical prototype.

### B. Numerical Experiments

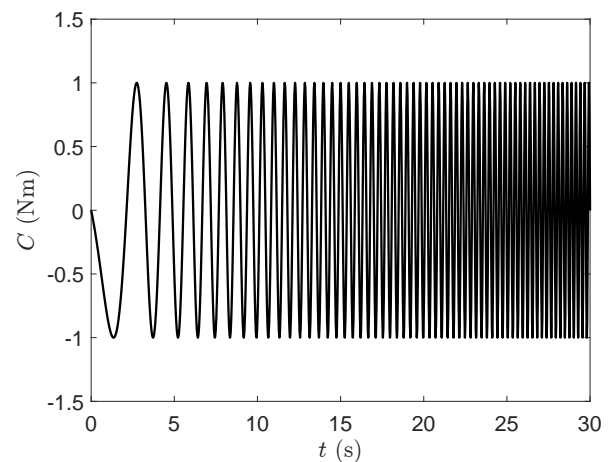
The latching mechanism is the articulated mechanical system analyzed in this work, as mentioned before. In this mechanism, the three latches can be latched and unlatched through a system of connecting elements maneuvered with a specific handle. In particular, the latching system has one degree of freedom. Namely, the rotation of the handle, which transmits the motion through a set of rods and shafts to the three latches, can be seen as the system degree of freedom represented in Figures 2 and 3.

To study the dynamic behavior of the latching mechanism, an appropriate torque is applied to the handle that controls the motion of the complete system. In particular, two diverse cases are analyzed for performing numerical experiments, in which two different types of time laws for the control torques are applied to the revolute joint that enables the handle to rotate. Moreover, all the dynamical simulations are performed in the presence of a gravitational acceleration  $g$  equal to  $9.81 \text{ (m/s}^2\text{)}$ . The time span considered for the numerical simulations is denoted with  $T_s$  and is equal to  $30 \text{ (s)}$ , while the time step is indicated as  $\Delta t$  and is equal to  $10^{-3} \text{ (s)}$ . In the first case, the applied torque is given by an impulse, that is, a high constant value of the torque is applied for a short amount of time to the handle of the

mechanism. In the second case, the torque law is represented as a sine sweep function, which is largely used in engineering applications for experimental testing and operational modal analysis [76]–[79]. In Figure 4, the two input signals used as torque laws are showed, namely, the impulse function is represented in Figure 4(a) and the sine sweep function is represented in Figure 4(b).



(a) Case 1: impulse function.

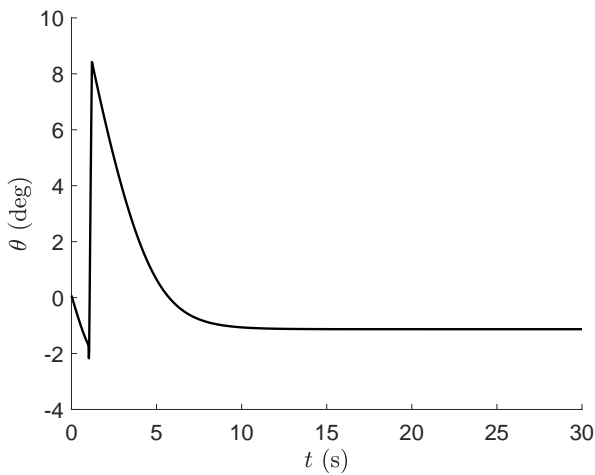


(b) Case 2: sine sweep function.

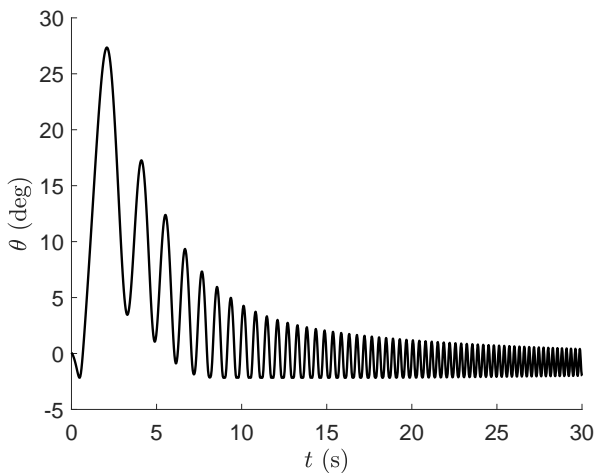
Fig. 4. Time laws of the torque inputs imposed on the latching mechanism.

In these two scenarios, the angular displacements of the three latches of the mechanism obtained through dynamical simulations carried out by using the multibody model developed from the mechanical design were recorded. In Figure 5, the numerical results for the two diverse input torques are graphically represented, namely, in Figure 5(a), the angular displacement of the latches in response to the impulse torque function is shown, while, in Figure 5(b), the angular displacement of the latches in response to the sine sweep torque function is shown.

As expected, the numerical results represented in Figure 5 show a strong relationship to the type of the inputs represented in Figure 4. The data gathered from the dynamical simulations described above can be used to identify a state-space model of the latching mechanism. The identification procedure is based on the computer implementation of the Numerical Algorithms for Subspace State-Space System Identification (N4SID), which was described previously in this work. Starting from the input data and the output



(a) Case 1: latches angular displacement in response to the impulse function.



(b) Case 2: latches angular displacement in response to the sine sweep function.

Fig. 5. Time laws of the angular displacements resulting from the latching mechanism.

measurements of a given dynamical simulation, a linear state-space model can be obtained using this computational approach for realizing the applied system identification. By using the data reported in Figures 4 and 5, respectively, as input and output data for the N4SID algorithm, it is possible to obtain the identification of two different state-space dynamical models. For simplicity, to clearly distinguish the numerical results found from the use of the system identification numerical procedure, the quantities related to the impulse input signal are referred to as the case 1. These quantities are accordingly identified by the subscript 1. On the other hand, the quantities related to the sine sweep input signal are referred to as the case 2. These quantities are accordingly identified by the subscript 2. The state-space matrices of the discrete dynamical model identified in the first case, namely for the impulse input and the corresponding output respectively shown in Figures 4(a) and 5(a), are the

following:

$$\left\{ \begin{array}{l} \mathbf{A}_{d,1} = \begin{bmatrix} 1 & -0.0001 \\ 0.0002 & 0.9996 \end{bmatrix} \\ \mathbf{B}_{d,1} = \begin{bmatrix} 0.1082 \cdot 10^{-3} \\ 0.1224 \cdot 10^{-3} \end{bmatrix} \\ \mathbf{C}_1 = [ -60.4670 \quad -170.9435 ] \\ \mathbf{D}_1 = 0.6 \end{array} \right. \quad (52)$$

The state-space matrices of the discrete dynamical model identified in the second case, namely for the sine sweep input and the corresponding output respectively shown in Figures 4(b) and 5(b), are the following:

$$\left\{ \begin{array}{l} \mathbf{A}_{d,2} = \begin{bmatrix} 1 & -0.0002 \\ 0.0070 & 0.9963 \end{bmatrix} \\ \mathbf{B}_{d,2} = \begin{bmatrix} -0.0567 \cdot 10^{-3} \\ -0.2621 \cdot 10^{-3} \end{bmatrix} \\ \mathbf{C}_2 = [ 703.5202 \quad -41.6898 ] \\ \mathbf{D}_2 = 0.0078 \end{array} \right. \quad (53)$$

Starting from the two discrete-time models, the continuous-time models can be found. In particular, the identified continuous-time state matrices and the identified continuous-time input influence matrices for the two cases can be defined by properly transforming their discrete-time formulation. For the first case, the continuous-time state matrix and the continuous-time input influence matrix, respectively denoted with  $\mathbf{A}_{c,1}$  and  $\mathbf{B}_{c,1}$ , are the following:

$$\left\{ \begin{array}{l} \mathbf{A}_{c,1} = \begin{bmatrix} 0.0129 & -0.0948 \\ 0.1692 & -0.3997 \end{bmatrix} \\ \mathbf{B}_{c,1} = \begin{bmatrix} 0.1082 \\ 0.1244 \end{bmatrix} \end{array} \right. \quad (54)$$

For the second case, the continuous-time state matrix and the continuous-time input influence matrix, respectively denoted with  $\mathbf{A}_{c,2}$  and  $\mathbf{B}_{c,2}$ , are the following:

$$\left\{ \begin{array}{l} \mathbf{A}_{c,2} = \begin{bmatrix} 0.445 & -0.1546 \\ 6.9941 & -3.7146 \end{bmatrix} \\ \mathbf{B}_{c,2} = \begin{bmatrix} -0.0568 \\ -0.2624 \end{bmatrix} \end{array} \right. \quad (55)$$

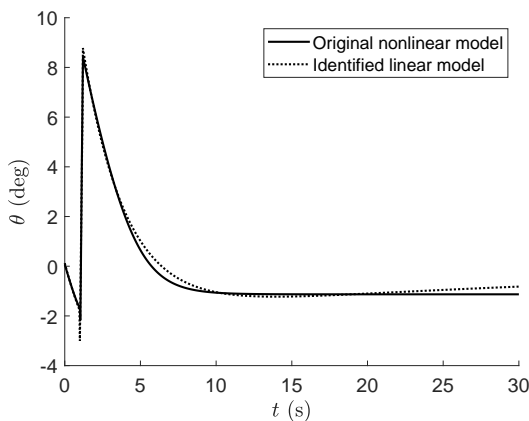
It is noteworthy mentioning that some useful information can be gained from the discrete-time and continuous-time state-space models identified in the two test cases considered in this investigation. In particular, in the two test cases, one can readily compute the two eigenvalues of the discrete-time state matrix, respectively denoted with  $\lambda_{I,d}$  and  $\lambda_{II,d}$ , the two eigenvalues of the continuous-time state matrix, respectively denoted with  $\lambda_{I,c}$  and  $\lambda_{II,c}$ , and the two time constants related to the continuous-time state-space models, respectively indicated as  $\tau_{I,c}$  and  $\tau_{II,c}$ . In Table I, these significant numerical results arising from the eigenvalue analysis of the identified state-space models obtained in the two cases considered in this paper are synthetically reported.

TABLE I

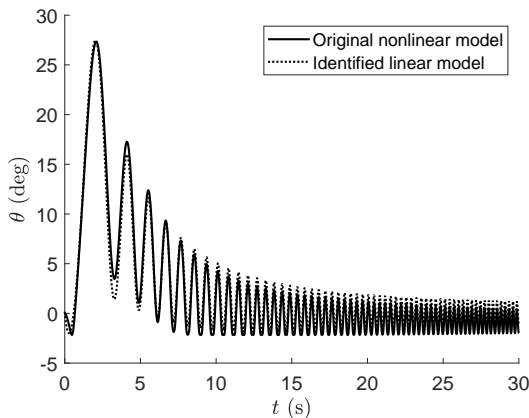
NUMERICAL RESULTS OF THE EIGENVALUE ANALYSIS CARRIED OUT FOR THE IDENTIFIED STATE-SPACE MODELS IN THE TWO DIFFERENT TEST CASES.

Test Case	$\lambda_{I,d}$	$\lambda_{II,d}$	$\lambda_{I,c}$	$\lambda_{II,c}$	$\tau_{I,c}$	$\tau_{II,c}$
Case 1	0.9999	0.9996	-0.0305	-0.3563	32.7546	2.8069
Case 2	0.9997	0.9966	-0.2695	-3.4007	3.7112	0.2941

To understand how close to the original multibody model are the dynamical behaviors of the identified linear dynamical models, the outputs of the multibody numerical simulations and the outputs of the identified linear models can be compared in the two different cases, namely the impulse function and the sine sweep function employed as input torques. To this end, the comparison of the identified linear dynamical models with the original nonlinear multibody model is represented in Figure 6.



(a) Case 1: comparison between the latch angular displacements when the input torque is an impulse function.



(b) Case 2: comparison between the latch angular displacements when the input torque is a sine sweep function.

Fig. 6. Comparison between the simulated original latch angular displacement and the latch angular displacement calculated with the identified state-space model in the two different cases. The solid lines represent the latch angular displacements calculated using the original multibody model. The dotted lines represent the latch angular displacement calculated using the identified state-space model.

In Figure 6(a), the nonlinear simulation of the multibody model and the linear simulation of the identified model are compared on the same graph in the case of the impulse function. Similarly, in Figure 6(b), the same comparison is made for the case of the sine sweep function. Since the numerical results represented in Figure 6 show a good

agreement between the identified and the original models, the effectiveness of using the identification method considered in this paper for obtaining a simple linear state-space approximation of a complex nonlinear multibody model is demonstrated.

To illustrate the practical application of the two state-space models identified in the two test cases considered herein, consider the discrete-time infinite-horizon optimal control problem. The solution to this problem originates from the computation of the unique stabilizing solution of the discrete-time algebraic Riccati equation. It allows for determining an optimal feedback matrix that stabilizes the corresponding closed-loop dynamical system. To demonstrate this fact through numerical experiments, consider the identified discrete-time state-space model found in the first test case, and assume the following weight matrices:

$$Q_{d,1} = \begin{bmatrix} 10^3 & 0 \\ 0 & 10^3 \end{bmatrix}, \quad R_{d,1} = 1 \quad (56)$$

where  $Q_{d,1}$  is the weight matrix for the state vector and  $R_{d,1}$  is the weight matrix for the vector of control inputs, both referred to the first test case. In the first test case, the solution of the discrete-time infinite-horizon optimal control problem is given by the following matrices:

$$\begin{cases} S_{d,1} = \begin{bmatrix} 1.3547 \cdot 10^6 & -0.9967 \cdot 10^6 \\ -0.9967 \cdot 10^6 & 1.0385 \cdot 10^6 \end{bmatrix} \\ F_{d,1} = [ 24.4610 \quad 19.1531 ] \end{cases} \quad (57)$$

where  $S_{d,1}$  is the stabilizing solution of the discrete-time algebraic Riccati equation and  $F_{d,1}$  is the corresponding optimal feedback gain matrix, both referred to the first test case. It follows that, in the first test case in which the impulse function was used as the input law to perform the identification process, the closed-loop state matrix becomes:

$$\bar{A}_{d,1} = A_{d,1} - B_{d,1}F_{d,1} = \begin{bmatrix} 0.9973 & -0.0022 \\ -0.0028 & 0.9972 \end{bmatrix} \quad (58)$$

where  $\bar{A}_{d,1}$  denotes the closed-loop state matrix obtained from the first test. Similarly, consider the identified discrete-time state-space model found in the second test case, and assume the following weight matrices:

$$Q_{d,2} = \begin{bmatrix} 10^3 & 0 \\ 0 & 10^3 \end{bmatrix}, \quad R_{d,2} = 1 \quad (59)$$

where  $Q_{d,2}$  is the weight matrix for the state vector and  $R_{d,2}$  is the weight matrix for the vector of control inputs, both referred to the second test case. In the second test case, the solution of the discrete-time infinite-horizon optimal control problem is given by the following matrices:

$$\begin{cases} S_{d,2} = \begin{bmatrix} 5.6612 \cdot 10^5 & -0.2106 \cdot 10^5 \\ -0.2106 \cdot 10^5 & 0.8182 \cdot 10^5 \end{bmatrix} \\ F_{d,2} = [ -26.5404 \quad -20.0337 ] \end{cases} \quad (60)$$

where  $S_{d,2}$  is the stabilizing solution of the discrete-time algebraic Riccati equation and  $F_{d,2}$  is the corresponding optimal feedback gain matrix, both referred to the second test case. It follows that, in the second test case in which the sine sweep function was used as the input law to perform the

identification process, the closed-loop state matrix becomes:

$$\bar{\mathbf{A}}_{d,2} = \mathbf{A}_{d,2} - \mathbf{B}_{d,2}\mathbf{F}_{d,2} = \begin{bmatrix} 0.9985 & -0.0013 \\ 0.0001 & 0.9910 \end{bmatrix} \quad (61)$$

where  $\bar{\mathbf{A}}_{d,2}$  denotes the closed-loop state matrix obtained from the second test.

Finally, to prove the consistency of the two closed-loop models obtained from the identification process carried out for the two test cases and subsequently associated with two different discrete-time optimal controllers, consider the following numerical experiment. Basically, the same external input law for the control torque is applied to both the two open-loop and closed-loop state-space models, and the resulting time responses are compared. The sinusoidal time law of the input torque used for performing this final test is represented in Figure 7.

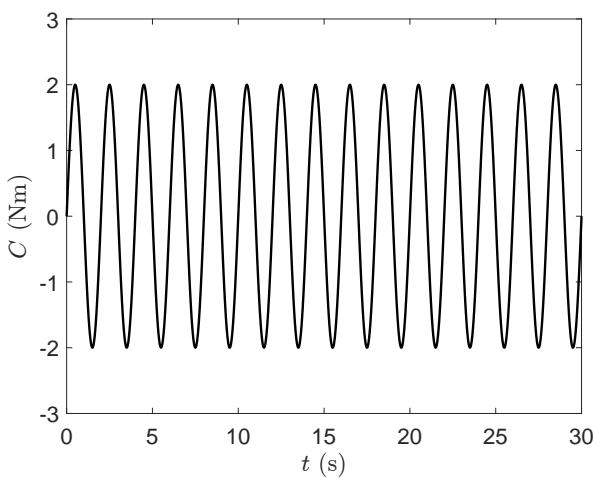


Fig. 7. Sinusoidal time law of the torque input imposed on the latching mechanism in the final test.

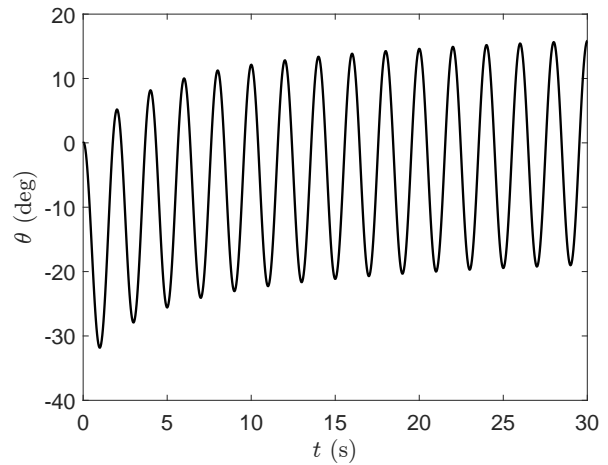
The time responses obtained from the open-loop models based on the identified state-space systems are represented in Figure 8, namely, in Figure 8(a), the system open-loop response to the sinusoidal input torque obtained from the first test case is shown, while, in Figure 8(b), the system open-loop response to the sinusoidal input torque obtained from the second test case is shown.

The time responses obtained from the closed-loop models based on the identified state-space systems are represented in Figure 9, namely, in Figure 9(a), the system closed-loop response to the sinusoidal input torque obtained from the first test case is shown, while, in Figure 9(b), the system closed-loop response to the sinusoidal input torque obtained from the second test case is shown.

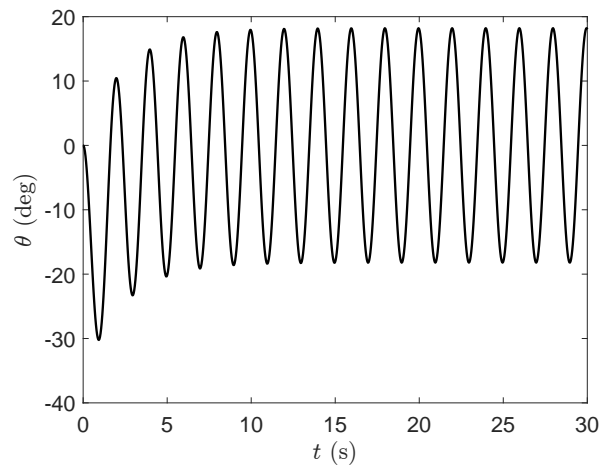
By observing Figures 8 and 9, it is apparent that the two different time responses associated with the closed-loop systems, obtained in the two test cases and by introducing the discrete-time optimal controller, are very similar, thereby demonstrating the usefulness of the identification process for the design of feedback control laws.

C. Final Remarks

The numerical results obtained in this section show the effectiveness of using the N4SID method as an algorithm to identify a linear state-space dynamical model of a complex



(a) Angular displacement of the open-loop model derived from the first test case (impulse function) in response to the sinusoidal torque.

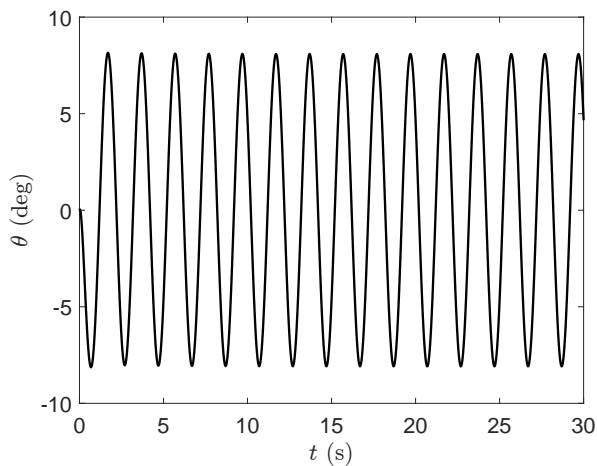


(b) Angular displacement of the open-loop model derived from the second test case (sine sweep function) in response to the sinusoidal torque.

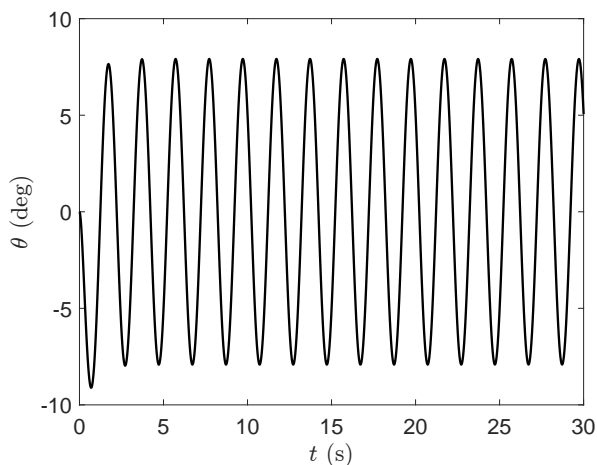
Fig. 8. Open-loop time responses of the state-space models identified for the latching mechanism in the final test.

mechanical system such as the latching mechanism considered in this work. In particular, all the numerical results presented herein are obtained through the use of the CVA variant of the family of the N4SID computational procedures. This was done based on input and output data obtained from the analysis of a multibody model instead of using a real prototype of the physical system of interest. Although the original system is clearly nonlinear, the algorithm allows for finding an acceptable linear approximation that describes well the behavior of the latching mechanism. The identified system is simpler and faster to use so that it could be further improved and used for control purposes.

The numerical results represented in Figure 6 shows how the identified system describes well the original system as the nonlinearity of the system starts to be negligible, and the same set of input excitation is used. In effect, this behavior can be seen in the first case of Figure 6(a), but it is definitely more clear in the case of the sine sweep excitation. In fact, in Figure 6(b), as the amplitude of the input torque decreases, and, consequently, the latch angular displacement reduces, the difference between the original nonlinear model and the identified linear model diminishes as well.



(a) Angular displacement of the closed-loop model derived from the first test case (impulse function) in response to the sinusoidal torque.



(b) Angular displacement of the closed-loop model derived from the second test case (sine sweep function) in response to the sinusoidal torque.

Fig. 9. Closed-loop time responses of the state-space models identified for the latching mechanism in the final test.

Finally, it is important to underline that the identified model is a simple black-box model based only on an input-output relationship. Therefore, for the purposes of the present work, there is no need to describe or to make any consideration about the physics of the problem. As shown in Figures 9 and 8, this is also demonstrated in this paper by considering the numerical experiments in which two different feedback controllers are designed using the two identified discrete-time state-space models. Since in both cases one obtains almost identical time responses, as shown in Figures 8(a), 8(b), 9(a), and 9(b), the identified models can be used with high confidence in the design process of feedback controllers.

#### IV. SUMMARY, CONCLUSIONS, AND FUTURE WORK

The research issues of prominent interest for the authors are system identification [80], [81], nonlinear control [82], [83], and multibody dynamics [84], [85]. The academic efforts of the authors, therefore, investigate the connections between these three apparently separated fields of research. This paper particularly focuses on applying computational system identification techniques for obtaining simplified dynamical models of complex mechanical systems

of engineering relevance, such as the latching system of an aircraft cargo hatch door. This work aims to show the possibility of identifying a simplified linear dynamical model of a complex mechanical system starting from its multibody model that is obtained through the integration of CAD and CAE systems to emulate the real physical behavior of the system of interest through numerical experiments performed using its virtual prototype. For this purpose, in the paper, the first step consisted of simplifying the CAD model of the latching system extracted from the ATR 42/72 cargo hatch door to develop a multibody model of the same mechanical system in the SIMSCAPE multi-domain environment of MATLAB. Subsequently, extensive numerical experiments were performed through computer simulations of the original nonlinear multibody model to capture some key features of the relevant dynamical behavior of the system.

Since the latching mechanism considered in this paper is a complex multibody system featuring one degree of freedom, the campaign of numerical experiments was done to obtain the system response in two scenarios, namely when the torque applied to the handle of the mechanism follows an impulse function and when the time law of the external torque is a sine sweep function, typically employed in operational modal analysis. Once the system response is acquired for the two cases mentioned before, a proper couple of input-output data set is established for the computer implementation of the Numerical Algorithms for Subspace State-Space System Identification (N4SID). Using this identification procedure, discrete-time and continuous-time state-space dynamical models are constructed for the two test cases to define a simple mathematical model of the complex mechanism of interest that is based on virtual experiments instead of real testing. In the two test cases, this process yields the identification of the system state matrix, the input influence matrix, the output influence matrix, and the direct transmission matrix. In particular, insight information can be found by performing an eigenvalue analysis of the identified state-space models so determined. The numerical results found as the outcome of the present identification process, therefore, allows for obtaining a simple linear approximation of the original nonlinear multibody model that, aside from being able to map the same input-output relationship of the original system, can be used for several engineering applications, such as those that require a quick prediction to estimate the system response, most of all, in control engineering systems.

Several interesting lines of research can be followed in future investigations. First, the use of other state-space identification algorithms based on time-domain data can be explored to understand if the outcome of the identification procedure in the case of nonlinear systems can still lead to useful numerical results representing a simplified linear approximation of the dynamical process to be captured. This strategy leverages the point that very often, in engineering practice, a nonlinear system must be analyzed and controlled only in a limited set of configurations or dynamical behaviors, thereby allowing for the use of simplified linear approximations. Furthermore, as mentioned in the paper, the principal goal behind the quest for a simplified model of a given mechanical system is the necessity to develop an effective control system capable of quickly adapting its

feedback behavior to the dynamics of the original systems to be controlled. This need is quite general and common for many mechanical systems such as robots, vehicles, machines, mechanisms, and structures. Another important point to be addressed in future works is the development and the practical use of an additional identification method capable of extracting the physical parameters of a mechanical system, like the system mass, stiffness, and damping matrices, from its identified state-space dynamical model. These issues will be addressed in future investigations.

#### AUTHORS' CONTRIBUTIONS

This research paper was principally developed by the first author (Carmine Maria Pappalardo). Great support was provided by the second author (Antonio Lettieri). The detailed review carried out by the third author (Domenico Guida) considerably improved the quality of the work. The manuscript was written through the contribution of all authors. All authors discussed the results, reviewed and approved the final version of the manuscript.

#### REFERENCES

- [1] A. A. Shabana, *Dynamics of Multibody Systems*, Cambridge University Press: New York, NY, USA, 2013.
- [2] A. A. Shabana, *Computational Dynamics*, John Wiley and Sons: The Atrium, Southern Gate, Chichester, West Sussex, UK, 2009.
- [3] R. F. Ribeiro, T. G. Ritto, H. F. Campos Velho, and J. Herskovits, "Damage identification in a multi-DOF system under uncertainties using optimization algorithms," *Journal of Applied and Computational Mechanics*, vol. 4, no.4, pp365-374, 2018.
- [4] N. Pnevmatikos, "Pole placement algorithm for control of civil structures subjected to earthquake excitation," *Journal of Applied and Computational Mechanics*, vol. 3, no.1, pp25-36, 2017.
- [5] H. Cho, "On Robust Adaptive PD Control of Robot Manipulators," *Journal of Applied and Computational Mechanics*, vol. 6, pp1450-1466, 2020.
- [6] A. Ajorkar, A. Fazlyab, F. Fani Saberi, and M. Kabganian, "Design of an adaptive-neural network attitude controller of a satellite using reaction wheels," *Journal of Applied and Computational Mechanics*, vol. 1, no.2, pp67-73, 2014.
- [7] P. Van Overschee and B. L. De Moor, *Subspace identification for linear systems: Theory-Implementation-Applications*, Springer Science and Business Media, 2012.
- [8] J. N. Juang, *Applied system identification*, Prentice-Hall, Upper Saddle River, New Jersey, USA, 1994.
- [9] L. Salvati, M. D'Amore, A. Fiorentino, A. Pellegrino, P. Sena, and F. Vilecco, "Development and Testing of a Methodology for the Assessment of Acceptability of LKA Systems," *Machines*, vol. 8, no.3, 47, 2020.
- [10] T. Li, Z. Kou, J. Wu, W. Yahya, and F. Vilecco, "Multipoint Optimal Minimum Entropy Deconvolution Adjusted for Automatic Fault Diagnosis of Hoist Bearing," *Shock and Vibration*, vol. 2021, 6614633, 2021.
- [11] A. Liguori, E. Armentani, A. Bertocco, A. Formato, A. Pellegrino, and F. Vilecco, "Noise Reduction in Spur Gear Systems," *Entropy*, vol. 22, no.11, 1306, 2020.
- [12] X. Sun, H. Liu, W. Song, and F. Vilecco, "Modeling of Eddy Current Welding of Rail: Three-Dimensional Simulation," *Entropy*, vol. 22, no.9, 947, 2020.
- [13] L. U. Gokdere, K. Benlyazid, R. A. Dougal, E. Santi, and C. W. Brice, "A virtual prototype for a hybrid electric vehicle," *Mechatronics*, vol. 12, no.4, pp575-593, 2002.
- [14] E. Grossi, C. J. Desai, and A. A. Shabana, "Development of Geometrically Accurate Continuum-Based Tire Models for Virtual Testing," *Journal of Computational and Nonlinear Dynamics*, vol. 14, no.12, 121006, 2019.
- [15] K. Lee, *Principle of CAD/CAM/CAE system*, Addison-Wesley Longman, Reading, Massachusetts, USA, 1999.
- [16] E. J. Haug, *Computer aided analysis and optimization of mechanical system dynamics*, Springer-Verlag, Berlin Heidelberg, 1984.
- [17] A. M. Ji, K. Zhu, J. C. Huang, and Y. P. Dong, "CAD/CAE integration system of mechanical parts," *Advanced Materials Research*, vol. 338, pp272-276, 2011.
- [18] C. Tierney, D. Nolan, T. Robinson, and C. Armstrong, "Using mesh-geometry relationships to transfer analysis models between CAE tools," *Engineering with Computers*, vol. 31, pp465-481, 2015.
- [19] Q. Feng, X. Zhou, and J. Li, "A hybrid and automated approach to adapt geometry model for CAD/CAE integration," *Engineering with Computers*, vol. 36, pp1-21, 2019.
- [20] A. Daberkow and E. J. Kreuzer, "An integrated approach for computer aided design in multibody system dynamics," *Engineering with Computers*, vol. 15, no.2, pp155-170, 1999.
- [21] M. Otter, M. Hocke, A. Daberkow, and G. Leister, "An object-oriented data model for multibody systems," *Advanced Multibody System Dynamics*, Springer, Dordrecht, pp19-48, 1993.
- [22] A. Thakur, A. G. Banerjee, and S. K. Gupta, "A survey of CAD model simplification techniques for physics-based simulation applications," *Computer-Aided Design*, vol. 41, no.2, pp65-80, 2009.
- [23] A. A. Shabana, "Integration of computer-aided design and analysis: application to multibody vehicle systems," *International Journal of Vehicle Performance*, vol. 5, no.3, pp300-327, 2019.
- [24] H. Shi, L. Wang, B. Nicolsen, and A. A. Shabana, "Integration of geometry and analysis for the study of liquid sloshing in railroad vehicle dynamics," *Proceedings of the Institution of Mechanical Engineers, Part K: Journal of Multi-body Dynamics*, vol. 231, no.4, pp608-629, 2017.
- [25] M. T. H. Khan and S. Rezwana, "A review of CAD to CAE integration with a hierarchical data format (HDF)-based solution," *Journal of King Saud University-Engineering Sciences*, In press, 2020.
- [26] O. Hamri, J. C. Leon, F. Giannini, and B. Falcidieno, "Software environment for CAD/CAE integration," *Advances in Engineering Software*, vol. 41, no.10-11, pp1211-1222, 2010.
- [27] T. Makkonen, K. Nevala, and R. Heikkila, "A 3D model based control of an excavator," *Automation in Construction*, vol. 15, no.5, pp571-577, 2006.
- [28] D. Cekus, B. Posiadala, and P. Warys, "Integration of Modeling in Solidworks and Matlab/Simulink Environments," *Archive of Mechanical Engineering*, vol. 61, no.1, pp57-74, 2014.
- [29] S. A. A. Adam, J. P. Zhou, and Y. H. Zhang, "Modeling and simulation of 5DOF robot manipulator and trajectory using MATLAB and CATIA," *3rd International Conference on Control, Automation and Robotics (ICCAR)*, Nagoya, pp36-40, 2017.
- [30] C. M. Pappalardo, N. Lombardi, and D. Guida, "A Model-Based System Engineering Approach for the Virtual Prototyping of an Electric Vehicle of Class L7," *Engineering Letters*, vol. 28, no.1, pp215-234, 2020.
- [31] G. P. Gujarathi and Y. S. Ma, "Parametric CAD/CAE integration using a common data model," *Journal of Manufacturing Systems*, vol. 30, no.3, pp118-132, 2011.
- [32] A. Mikkola, A. A. Shabana, C. Sanchez-Rebollo, and J. R. Jimenez-Octavio, "Comparison between ANCF and B-spline surfaces," *Multibody System Dynamics*, vol. 30, no.2, pp119-138, 2013.
- [33] D. F. Rogers, *An introduction to NURBS: with historical perspective*, Morgan Kaufmann Publishers, San Francisco, California, USA, 2001.
- [34] W. Schiehlen, *Advanced multibody system dynamics: Simulation and Software tools*, Springer Science and Business Media, 2013.
- [35] S. Kwon, B. C. Kim, D. Mun, and S. Han, "Simplification of feature-based 3D CAD assembly data of ship and offshore equipment using quantitative evaluation metrics," *Computer-Aided Design*, vol. 59, pp140-154, 2015.
- [36] X. Liu, X. Yang, P. Zhu, and W. Xiong, "Robust identification of nonlinear time-delay system in state-space form," *Journal of the Franklin Institute*, vol. 356, no.16, pp9953-9971, 2019.
- [37] G. G. Wang, "Definition and review of virtual prototyping," *Journal of Computing and Information Science in Engineering*, vol. 2, no.3, pp232-236, 2002.
- [38] J. C. Kunz, T. R. Christiansen, G. P. Cohen, Y. Jin, and R. E. Levitt, "The virtual design team," *Communications of the ACM*, vol. 41, no.11, pp84-91, 1998.
- [39] Y. W. D. Tay, B. Panda, S. C. Paul, N. A. Noor Mohamed, M. J. Tan, and K. F. Leong, "3D printing trends in building and construction industry: a review," *Virtual and Physical Prototyping*, vol. 12, no.3, pp261-276, 2017.
- [40] A. Z. Sampaio, M. M. Ferreira, D. P. Rosario, and O. P. Martins, "3D and VR models in Civil Engineering education: Construction, rehabilitation and maintenance," *Automation in Construction*, vol. 19, no.7, pp819-828, 2010.
- [41] F. Farroni and F. Timpone, "A Test Rig for Tyre Envelope Model Characterization," *Engineering Letters*, vol. 24, no.3, pp290-294, 2016.
- [42] F. Renno and M. Terzo, "Close-range photogrammetry approach for the virtual prototyping of an automotive magnetorheological semi-active differential," *Engineering letters*, vol. 23, no.3, pp163-172, 2015.

- [43] P. K. Collins, R. Leen, and I. Gibson, "Industry case study: rapid prototype of mountain bike frame section," *Virtual and Physical Prototyping*, vol. 11, no.4, pp295-303, 2016.
- [44] F. Renno and S. Papa, "Direct Modeling Approach to Improve Virtual Prototyping and FEM Analyses of Bicycle Frames," *Engineering Letters*, vol. 23, no.4, pp333-341, 2015.
- [45] B. Camburn, B. Dunlap, T. Gurjar, C. Hamon, M. Green, D. Jensen, R. Crawford, K. Otto, and K. Wood, "A systematic method for design prototyping," *Journal of Mechanical Design*, vol. 137, no.8, 081102, 2015.
- [46] C. M. Pappalardo and D. Guida, "Dynamic Analysis and Control Design of Kinematically-Driven Multibody Mechanical Systems," *Engineering Letters*, vol. 28, no.4, pp1125-1144, 2020.
- [47] D. Amodio, M. Callegari, P. Castellini, A. Crivellini, G. Palmieri, M. C. Palpacelli, N. Paone, M. Rossi, and M. Sasso, "Integrating Advanced CAE Tools and Testing Environments for the Design of Complex Mechanical Systems," *The First Outstanding 50 Years of "Università Politecnica delle Marche"*, Springer, Cham, pp247-258, 2019.
- [48] Q. Tian, P. Flores, and H. M. Lankarani, "A comprehensive survey of the analytical, numerical and experimental methodologies for dynamics of multibody mechanical systems with clearance or imperfect joints," *Mechanism and Machine Theory*, vol. 122, pp. 1-57, 2018.
- [49] P. Flores, "Concepts and formulations for spatial multibody dynamics," Springer International Publishing, 2015.
- [50] F. Aghili, "A unified approach for inverse and direct dynamics of constrained multibody systems based on linear projection operator: applications to control and simulation," *IEEE Transactions on Robotics*, vol. 21, no.5, pp834-849, 2005.
- [51] W. Rulka and E. Pankiewicz, "MBS approach to generate equations of motions for HiL-simulations in vehicle dynamics," *Multibody system dynamics*, vol. 14, no.3-4, pp367-386, 2005.
- [52] K. J. Keesman, *System Identification*, Springer, London, UK, 2011.
- [53] I. I. Lazaro, A. Alvarez, and J. Anzurez, "The Identification Problem Applied to Periodic Systems Using Hartley Series," *Engineering Letters*, vol. 21, no.1, pp36-43, 2013.
- [54] O. V. Chernoyarov, A. V. Zakharov, A. P. Trifonov, A. V. Salmikova, and A. A. Makarov, "The Common Approach to Calculating the Characteristics of the Signal Parameters Joint Estimates under the Violation of the Decision Statistics Regularity Conditions," *Engineering Letters*, vol. 28, no.2, pp492-503, 2020.
- [55] S. Gres, M. Dohler, P. Andersen, and L. Mevel, "Kalman filter-based subspace identification for operational modal analysis under unmeasured periodic excitation," *Mechanical Systems and Signal Processing*, vol. 146, 106996, 2020.
- [56] C. M. Pappalardo, A. Lettieri, and D. Guida, "Stability analysis of rigid multibody mechanical systems with holonomic and nonholonomic constraints," *Archive of Applied Mechanics*, vol. 90, no.9, pp1961-2005, 2020.
- [57] A. Cammarata and C. M. Pappalardo, "On the use of component mode synthesis methods for the model reduction of flexible multibody systems within the floating frame of reference formulation," *Mechanical Systems and Signal Processing*, 142, 106745, 2020.
- [58] M. Y. Karelina, E. Krylov, C. Rossi, S. Savino, and F. Timpone, "A Multibody Model of Federica Hand," *Engineering Letters*, vol. 24, no.4, pp406-417, 2016.
- [59] L. Ljung, R. Pintelon, and J. Schoukens, "System Identification: Wiley Encyclopedia of Electrical and Electronics Engineering," *System identification: a frequency domain approach*, John Wiley and Sons, no.2012, pp1-19, 1999.
- [60] J. N. Juang and M. Q. Phan, *Identification and control of mechanical systems*, Cambridge University Press, Cambridge, UK, 2001.
- [61] T. Katayama, *Subspace methods for system identification*, Springer Science and Business Media, London, UK, 2006.
- [62] C. M. Pappalardo and D. Guida, "System Identification and Experimental Modal Analysis of a Frame Structure," *Engineering Letters*, vol. 26, no.1, pp56-68, 2018.
- [63] T. S. Nord, O. W. Petersen, and H. Hendrikse, "Stochastic subspace identification of modal parameters during ice-structure interaction," *Philosophical Transactions of the Royal Society A*, vol. 377, no.2155, 20190030, 2019.
- [64] A. Lettieri and C. M. Pappalardo, "Experimental Identification of a Car Dynamic Model Using the Numerical Algorithms for Subspace State-Space System Identification," *Design, Simulation, Manufacturing: The Innovation Exchange*, Springer, Cham, pp14-23, 2020.
- [65] N. I. Zhiyu, L. I. U. Jinguo, W. U. Zhigang, and S. H. E. N. Xinhui, "Identification of the state-space model and payload mass parameter of a flexible space manipulator using a recursive subspace tracking method," *Chinese Journal of Aeronautics*, vol. 32, no.2, pp513-530, 2019.
- [66] P. Navik, A. Ronnquist, and S. Stichel, "Identification of system damping in railway catenary wire systems from full-scale measurements," *Engineering Structures*, vol. 113, pp71-78, 2016.
- [67] D. Yu, Y. Wang, H. Liu, K. Jermsittiparsert, and N. Razmjoo, "System identification of PEM fuel cells using an improved Elman neural network and a new hybrid optimization algorithm," *Energy Reports*, vol. 5, pp1365-1374, 2019.
- [68] H. Chen, L. Huang, L. Yang, Y. Chen, and J. Huang, "Model-based method with nonlinear ultrasonic system identification for mechanical structural health assessment," *Transactions on Emerging Telecommunications Technologies*, e3955, pp1-15, 2020.
- [69] W. S. Gray, G. S. Venkatesh, and L. A. D. Espinosa, "Nonlinear system identification for multivariable control via discrete-time Chen-Fliess series," *Automatica*, vol. 119, 109085, 2020.
- [70] R. T. Wu and M. R. Jahanshahi, "Data fusion approaches for structural health monitoring and system identification: past, present, and future," *Structural Health Monitoring*, vol. 19, no.2, pp552-586, 2020.
- [71] S. Klus, F. Nuske, S. Peitz, J. H. Niemann, C. Clementi, and C. Schutte, "Data-driven approximation of the Koopman generator: Model reduction, system identification, and control," *Physica D: Nonlinear Phenomena*, vol. 406, 132416, 2020.
- [72] L. Ljung, T. Chen, and B. Mu, "A shift in paradigm for system identification," *International Journal of Control*, vol. 93, no.2, pp173-180, 2020.
- [73] Z. Bai, E. Kaiser, J. L. Proctor, J. N. Kutz, and S. L. Brunton, "Dynamic mode decomposition for compressive system identification," *AIAA Journal*, vol. 58, no.2, pp561-574, 2020.
- [74] F. L. Zhang, S. K. Au, and Y. C. Ni, "Two-stage Bayesian system identification using Gaussian discrepancy model," *Structural Health Monitoring*, 1475921720933523, 2020.
- [75] A. H. Ribeiro, K. Tiels, J. Umenberger, T. B. Schon, and L. A. Aguirre, "On the smoothness of nonlinear system identification," *Automatica*, vol. 121, 109158, 2020.
- [76] G. Gloth and M. Sinapius, "Analysis of swept-sine runs during modal identification," *Mechanical systems and signal processing*, vol. 18, no.6, pp1421-1441, 2004.
- [77] T. Dossogne, L. Masset, B. Peeters, and J. P. Noel, "Nonlinear dynamic model upgrading and updating using sine-sweep vibration data," *Proceedings of the Royal Society A*, vol. 475, no.2229, 20190166, 2019.
- [78] E. Sauther, "Sine Sweep Vibration Testing for Modal Response Primer," *Department of Optical Sciences, University of Arizona, Tucson*, 2013.
- [79] C. Braccisi, F. Cianetti, L. Goracci, and M. Palmieri, "Sine-Sweep qualification test for engine components: The choice of simulation technique," *Procedia Structural Integrity*, vol. 24, pp360-369, 2019.
- [80] M. C. De Simone and D. Guida, "Experimental Investigation on Structural Vibrations by a New Shaking Table," *Conference of the Italian Association of Theoretical and Applied Mechanics*, Springer, Cham, pp819-831, 2019.
- [81] F. Colucci, M. C. De Simone, and D. Guida, "TLD design and development for vibration mitigation in structures," *International Conference New Technologies, Development and Applications*, Springer, Cham, pp59-72, 2019.
- [82] R. Guida, M. C. De Simone, P. Dasic, and D. Guida, "Modeling techniques for kinematic analysis of a six-axis robotic arm," *IOP Conference Series: Materials Science and Engineering*, IOP Publishing, vol. 568, no.1, 012115, 2019.
- [83] M. C. De Simone and D. Guida, "Control design for an under-actuated UAV model," *FME Transactions*, vol. 46, no.4, pp443-452, 2018.
- [84] Z. B. Rivera, M. C. De Simone, and D. Guida, "Unmanned ground vehicle modelling in Gazebo/ROS-based environments," *Machines*, vol. 7, no.2, 42, 2019.
- [85] C. M. Pappalardo, M. C. De Simone, and D. Guida, "Multibody modeling and nonlinear control of the pantograph/catenary system," *Archive of Applied Mechanics*, vol. 89, no.8, pp1589-1626, 2019.